PCCP

Accepted Manuscript

This is an *Accepted Manuscript*, which has been through the Royal Society of Chemistry peer review process and has been accepted for publication.

Accepted Manuscripts are published online shortly after acceptance, before technical editing, formatting and proof reading. Using this free service, authors can make their results available to the community, in citable form, before we publish the edited article. We will replace this *Accepted Manuscript* with the edited and formatted *Advance Article* as soon as it is available.

You can find more information about *Accepted Manuscripts* in the Information for Authors.

ROYAL SOCIETY OF CHEMISTRY

www.rsc.org/pccp

Chemical Science

ARTICLE

Illustrating the formation of metal nanoparticles with a growth concept based on colloidal stability

M. Wuithschick,[a] S. Witte,[a] F. Kettemann,[a] K. Rademann[a] and J. Polte[a]

A large number of scientific contributions is dedicated to the syntheses, characterization and applications of metal nanoparticles. In contrast, only few studies on their formation mechanisms have been reported. In general, concepts to describe particle growth processes are rare. Commonly used models are not able to explain the influences of reaction parameters on the growth and the final particle size. In this contribution it is shown how the growth of colloidal metal nanoparticles can be illustrated using an approach based on colloidal stability. In the first part, investigations of various syntheses of colloidal nanoparticles (including Rh, Pd, Pt, Cu, Ag, Au) show that growth due to aggregation and coalescence is the governing principle of nanoparticle formation if the monomer supply is faster than the actual growth. In the second part of this contibution, the influences of various parameters on the growth of Au nanoparticles are studied and it is demonstrated how the colloidal stability approach can illustrate the impact of synthesis parameters on the final particle size.

Introduction

In the last decades, metal nanoparticles have attracted considerable attention due to their unique properties.[1–3] Much effort was put into the development of synthetic strategies to produce nanoparticles of different sizes and morphologies often without understanding the underlying particle growth mechanisms.[4] Theoretical models to describe particle growth processes are rare[5–7] and they are hardly able to explain how synthesis parameters influence the final particle size or morphology.[8] Recently, a novel approach to illustrate growth processes of metal nanoparticles has been introduced.[9] This approach is based on colloidal rather than thermodynamic stability as for example in the widely-used LaMer nucleation and growth model.[10] The aim of this contribution is to give a general mechanistic survey of syntheses with $NaBH_4$ as reducing agent and to demonstrate the validity and the benefits of this novel growth concept with extensive experimental investigations.

Colloidal stability can be described as a sum of attractive and repulsive forces according to thetheory by Derjaguin, Landau, Verwey, Overbeek (known as DLVO theory).[11,12] The herein described colloids are electrostatically stabilized. Thus, the colloidal stability results from attractive van der Waals and repulsive electrostatic forces between the particles.[13,14] Figure 1a displays schematically the interaction energy between two identical spherical particles with dependence on their distance. The maximum of that curve (following denoted as aggregation barrier) represents the minimum thermal energy of two interacting particles which is necessary to induce their aggregation. The aggregation barrier provides a measure for the colloidal stability. In most cases, the aggregation barrier between two electrostatically stabilized particles increases with increasing particle size (displayed in Figure 1b and c); in other words, colloidal stability increases with increasing particle size. As long as a system provides enough thermal energy E_{kT} (E_{kT} > aggregation barrier), two particles can overcome the electrostatic repulsion and aggregate or coalesce, thus enabling nanoparticle growth. Figure 1c illustrates this approach in a simplified image. It shows an anticipated increase of the aggregation barrier between identical particles with respect to particle size. In this contribution, this curve is denoted as stability curve. E_{kt} separates the stability curve into two sections: In section I, the thermal energy is higher than the aggregation barrier. Thus, two particles can aggregate/coalesce and therefore grow. The growth process continues until section II is reached. At this point, the aggregation barrier cannot be overcome any longer inhibiting further particle growth. A stable colloidal solution is obtained. Simplified, the minimum final particle radius of the colloids is related to the intercept point of E_{kT} and the stability curve. Therefore, the final particle size of a colloidal solution is determined by (i) the stability curve which depends on the surface charge and therefore on the chemical composition of the colloidal solution and (ii) by the available thermal energy E_{kT}.

[a.] Humboldt-Universität zu Berlin, Department of Chemistry, Brook-Taylor-Str. 2, 12489 Berlin (Germany)
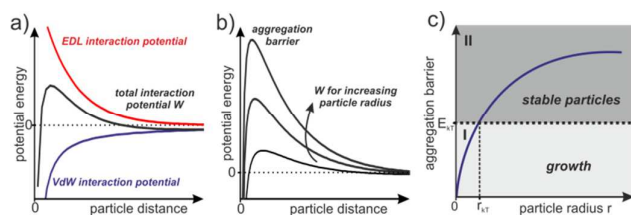
Figure 1. *Basic concept of nanoparticle growth based on colloidal stability for syntheses with a monomer supply faster than the actual particle growth.[9] a) Interaction potential between two identical spherical particles with their dependence on the particle distance due to the concept of electrostatic stabilization. b) Total interaction potential between two identical spherical particles with dependence on the particle distance for different particle radii. c) Concept of nanoparticle growth with colloidal stable particles being obtained at the intersection of E_{kT} and stability curve.*

In this contribution, syntheses of different metal nanoparticles with NaBH$_4$ as reducing agent are studied. The systems comprise a very fast reduction of the metal precursor so that monomer supply and actual particle growth are separated. The nanoparticles are colloidally stabilized due to electrostatic repulsion forces. Steric stabilization or covalent bonding of ligands does not have to be taken into account. In the first part of this work, it is shown that growth due to aggregation or coalescence is a general principle of nanoparticle growth if the monomer supply is faster than the actual growth. In the second part, the influences of reaction conditions (cation, ionic strength, temperature) on the growth of gold nanoparticles are investigated. The results of this parameter study are discussed using the colloidal stability growth concept. The experimental results of both parts (i.e. the growth mechanisms as well as parameter influences) can be described and understood using the novel growth concept.

Growth driven by coalescence

Recently, time-resolved SAXS, XANES and UV-vis studies revealed for the reduction of tetrachloroauric acid (HAuCl$_4$) with sodium borohydride (NaBH$_4$) that nanoparticle growth is only due to coalescence.[15] The formation of silver nanoparticles (AgNP) obtained by the reduction of silver perchlorate (AgClO$_4$) with NaBH$_4$ was shown to be similar but with two well separated steps of coalescence.[16,17] Metastable particles with a mean radius of 2.3 nm are formed within 2 s. After full conversion of residual BH$_4^-$ to B(OH)$_4^-$, a second growth step is initiated. The molar ratios of metal precursor/reducing agent in the recent studies were 1:4 and 1:6 for the AuNP and AgNP synthesis, respectively.

For the herein discussed syntheses with a fast reduction, the novel growth concept claims that growth is only due to aggregation and coalescence.[9] To prove the validity of this growth principle, the growth mechanisms of several colloidal

nanoparticles syntheses including the reduction of aqueous HAuCl$_4$, NH$_4$AuCl$_4$, KAuCl$_4$, AgNO$_3$, Ag(CH$_3$COO), RhCl$_3$, H$_2$PtCl$_6$, Pd(NO$_3$)$_2$, Na$_2$PdCl$_4$, CuSO$_4$, Cu(CH$_3$COO)$_2$, Cu(NO$_3$)$_2$ and Cu(ClO$_4$)$_2$ solution with NaBH$_4$ at a molar ratio of 1:6 were investigated. Time-resolved UV-vis spectroscopy and small angle X-ray scattering (SAXS) were used to monitor the particle growth. A Continuous Flow Setup (CFS setup) was used for SAXS investigations to track nanoparticle growth for reaction times of t = 100 ms − 5 s. UV-vis spectra were collected between 300 ms and 5 s using a Stopped Flow Setup. The growth process between 15 s and 2 h was monitored with SAXS and UV-vis by taking aliquots of colloidal solution from a stirred batch reactor at different reaction times. Details on all experimental setups and procedures, information on the modelling of experimental SAXS data, selected scattering curves with corresponding mathematical fits and UV-vis spectra can be found in the Supporting Information (SI-1). Figure 2 displays the experimental results of SAXS investigations for the reduction of AgNO$_3$, CuSO$_4$ and Na$_2$PdCl$_4$. These three systems comprise different growth characteristics which are representative for all investigated systems.

The particle mean radii and the relative volume fractions (normalized to the last data point of the according system) are shown for 100 ms - 5 s (Figure 2a) and 15 s - 2 h (Figure 2b). For all syntheses, the first available data point was at t = 100 ms. For all three syntheses the particles grow in the first 5s to a metastable size. The article mean radii range from 1.2 nm (Pd), 1.8 nm (Ag) to 2.1 nm (Cu).. The polydispersity is constantly at 30 %. For all three syntheses, the relative volume fraction which embodies the total volume of all particles is almost constant between 100 ms and 5 s. It can be concluded that the metal precursors are reduced completely within the first 100 ms and that subsequent particle growth is not related to further reduction of the metal salts. Therefore, particle growth is due to coalescence of primary formed clusters. The results of the SAXS investigations between 15 s and 2 h show clear similarities to the reduction of AgClO$_4$ with NaBH$_4$.[16] After a phase of approx. 30 min during which the size distribution remains almost constant (denoted as metastable state) a second growth step is observed. For Ag, the mean radius increases to 5.0 nm (polydispersity 20 %). The final colloidal solution is stable for weeks. The Cu nanoparticles grow fast to micrometer size and precipitate during the second growth step. The Pd particles reach a size of approx. 2.5 nm (polydispersity 30 %) after 2 h. They slowly grow further and precipitate after some days. For all investigated systems, the volume fraction is the same before and after the second growth step (for Cu until precipitation is observed) which indicates that the second growth step is also governed by coalescence. The other investigated systems of metal nanoparticles (see results and discussion in SI-2) show the same characteristic of two separated steps of coalescence.
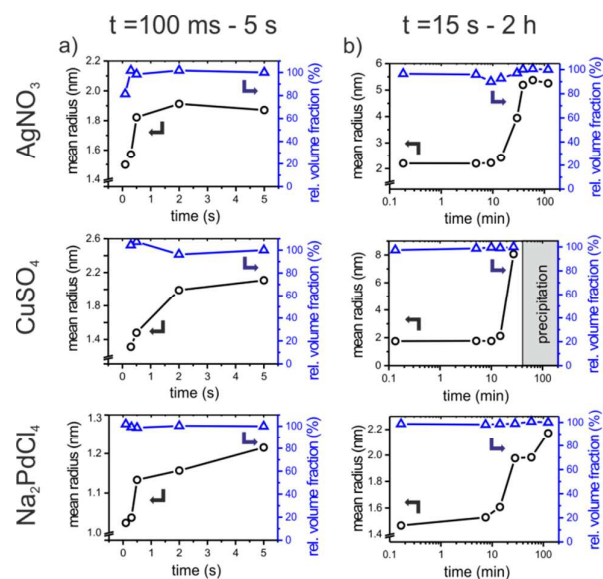
Figure 2. Results of time-resolved SAXS investigations of the growth of silver, copper and palladium nanoparticles synthesized by the reduction of different metal precursors with $NaBH_4$ at room temperature. a) Mean radius and relative volume fraction normalized to the last data point versus time for $t = 100$ ms $- 5$ s. b) Mean radius and relative volume fraction (normalized to the last data point) versus time for $t = 15$ s $- 2h$. Polydispersity is constantly 30% except for $AgNO_3$ in b) (20%).

In summary, the principle growth mechanism of nanoparticles using a variety of different metal precursors and $NaBH_4$ as reducing agent is similar to $AgClO_4/NaBH_4$. The metal ions are completely reduced by the reducing agent within less than 100 ms which means that the monomer supply is extremely fast – faster than the actual particle growth process. The monomers form dimers, trimers and so on to give small clusters which coalesce and form small nanoparticles with a minimal stable radius $\geq r_1$ whereby the value of r_1 depends on the system. During a metastable state, residual BH_4^- is converted to $B(OH)_4^-$ in the colloidal solution. The chemical conversion initiates a second step of coalescence[16] which can lead to three different scenarios; (i) long-term stable nanoparticles with mean radii between approx. 2-5 nm are formed; (ii) metastable nanoparticles with mean radii between approx. 2-3 nm are formed, the particles are not long-term stable and grow slowly further; or (iii) the particles exceed the length scale of nanoparticles and even precipitate during the second coalescent step. Systems which can be assigned to (i) are $HAuCl_4$, $AgNO_3$, $Ag(CH_3COO)$ and $AgClO_4/NaBH_4$. Group (ii) comprises the systems $KAuCl_4$, NH_4AuCl_4, Na_2PdCl_4, K_2PdCl_4 (see results of recent studies[18]), $Pd(NO_3)_2$, H_2PtCl_6 and $RhCl_3/NaBH_4$. Group (iii) includes $CuSO_4$, $Cu(NO_3)_2$, $Cu(CH_3COO)_2$, $Cu(ClO_4)_2/NaBH_4$. The growth mechanism of $HAuCl_4/NaBH_4$ deduced in an earlier publication (different reactant concentrations: 0.5 mM $HAuCl_4$ and 2 mM $NaBH_4$) is not in contradiction to the principle growth mechanism described herein although it comprises only one step of coalescence.[15] In that case the formed nanoparticles are not

affected by the conversion of BH_4^- since almost the entire amount of borohydride is already converted during the Au^{3+} reduction process. It could be said that the two coalescent steps are merged. The same effect is observed for other syntheses, e.g. the $AgClO_4/NaBH_4$ system.[17] With increasing excess of borohydride, a metastable state and a second coalescent growth step is also observed for the $HAuCl_4/NaBH_4$ system. The duration of the metastable phase depends on the molar ratio between gold precursor and reducing agent (see SI-3 for a concentration variation of the $HAuCl_4/NaBH_4$ synthesis).

In the picture of the growth concept, the first coalescent step ($t < 5$ s) can be illustrated with stability curve A in Figure 2a. Particles grow due to coalescence to a stable size slightly larger than the minimal radius r(A). After the first coalescent step, residual BH_4^- converts to $B(OH)_4^-$ within several minutes.[17] This change of the solution's chemical composition, change the surface chemistry (probably due to an oxidation process) which "decreases" the colloidal stability. This can be depicted with a change of the particle's stability curve while E_{kT} remains constant throughout the entire synthesis. The aggregation barrier of former stable particles with radii slightly larger than r(A) drops below E_{kT}. As a result, the particles aggregate or coalesce a second time until reaching a stable size again (intersection of E_{kT} and the new stability curve). The stability curve B in Figure 3a illustrates the growth for syntheses of group (i), the particles reach a stable size slightly above the minimal radius r(B). For group (ii) systems, particles coalesce until they reach a stable radius slightly above r(C). However, the new stability curve is close to E_{kT} which allows a slow continuous further growth (illustrated by system C in Figure 3a) or the process that leads to a decrease of colloidal stability is a rather slow process (i.e. surface oxidation) leading to a continuous variation of the stability curve. For this group, decreasing the temperature or adding a steric stabilizing agent to the particle solution can increase the difference between the stability curve of the system and E_{kT}, preventing further growth.[19] For group (iii) syntheses, the new stability curve is below E_{kT} for all particle radii in the nanoparticle length scale (illustrated by system D in Figure 3a). Therefore, stable colloidal nanoparticles are not obtained and particles even precipitate.
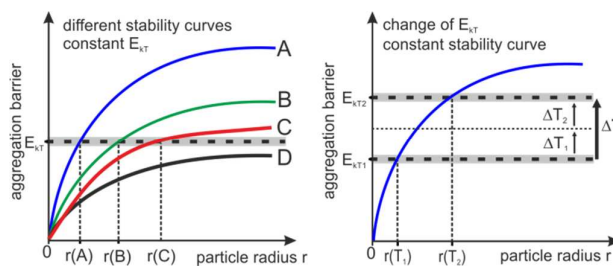

Figure 3. Schmeatic illustration of particle growth and parameter influences by the colloidal stability concept for a change of a) the stability curve and b) the thermal energy E_{kT}.

Influence of reaction parameters on the growth of Au nanoparticles

Common models describing metal colloidal growth are focused on the initial phase of nanoparticle formation. These models consider a phase of nuclei formation and its kinetics as size-determining step of a synthesis, for example the LaMer model which is based on the classical nucleation theory.[10] This approach is, however, not able to explain or even predict the influences of reaction parameters on the final size.[8] The growth concept depicted herein assumes that the final size is a matter of colloidal stability of the final colloidal solution and the influences of reaction conditions on the size can be described by their influence on the stability curves of a system.[9] In the simplified picture of this growth concept, the minimal final particle size is determined by the intersection of stability curve and available thermal energy E_{kT}. Therefore, the final size is affected by all parameters which determine the stability curve (such as ionic species or ionic strength[12]) or by a change of E_{kT} (temperature variation). To examine these influences, a parameter study with AuNP was performed. AuNP are a suitable model system since they are much less sensitive to external parameters (humidity, air pressure, dissolved oxygen etc.) than other metals, the syntheses are reproducible and lead to relatively monodisperse and stable nanoparticles. The reduction of $AuCl_4^-$ (0.5 mM) with $NaBH_4$ (2 mM) at 1:1 mixing was used to investigate the influences of cation species, ionic strength and temperature on the AuNP growth. Details of the synthetic procedures of the parameter study can be found in SI-4. All particle size distributions were determined with SAXS.

The cation influence was investigated using $HAuCl_4$, $KAuCl_4$ and NH_4AuCl_4 as gold precursors. The synthesis with H^+ comprises one step of coalescence whereas for K^+ and NH_4^+, two steps of coalescence are observed (see SI-5). The final particle mean radii after 2 h using H^+ and K^+ as counter ions are similar (1.9 and 2.1 nm) while NH_4^+ leads to larger particles with a mean radius of 4.3 nm. For mixtures of different precursors, the final particle sizes are congruent to calculations from their percentage ratios (see for example mixtures of $HAuCl_4/KAuCl_4$ or $HAuCl_4/NH_4AuCl_4$ in Figure 4a). Results of further binary and ternary precursor mixtures are included in SI-5.

The influence of ionic strength on the final size was investigated by addition of NH_4Cl and KCl. The salts were added in different concentrations to the three different gold precursors prior to the reduction with $NaBH_4$. Figure 4b shows the final mean radii versus concentration of added NH_4Cl (the results for addition of KCl are shown in SI-8). The final particle size is almost not affected by salt addition up to $[NH_4Cl] = 1$ mM. With increasing salt concentration above 1 mM, the final particle size increases. Precipitation of macroscopic gold is observed at a NH_4Cl concentration of 10 mM ($KAuCl_4$ precursor) or 100 mM ($HAuCl_4$ and NH_4AuCl_4 precursors), respectively. In a second experiment, the ionic strength of a colloidal solution was

increased subsequently to the synthesis (after 2 h). Figure 4b shows the final mean radii versus concentration of added NH_4Cl for salt addition subsequent to the particle synthesis from the $HAuCl_4$ precursor (orange data points). The results are almost identical to the results obtained from NH_4Cl addition prior to the synthesis (blue data points).

The influence of thermal energy on the growth was investigated with different synthesis temperatures and subsequent heating procedures. In one study, the synthesis temperature was varied between 1 and 80 °C. In a second study, a final colloidal solution synthesized at room temperature was subsequently heated with different heating procedures to 80 °C. Figure 4c shows the particle size versus synthesis temperature after 5 min. The mean radius increases from 1.2 nm (1 °C) to approx. 2.6 nm (80 °C). Heating of the colloidal solution subsequent to synthesis at standard conditions shows the same trend and almost the same results regardless of whether the solution is heated from room temperature to 80 °C in one step (green data points) or in many steps well separated in time (red data points).
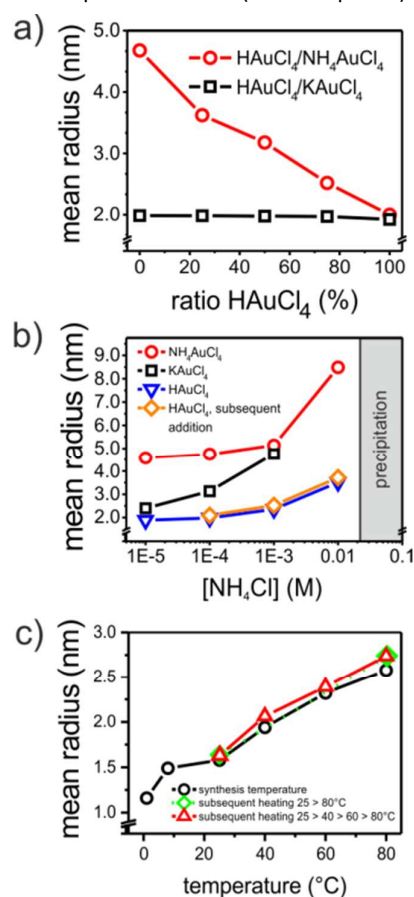

Figure 4. Results of parameter variation study for reduction of $AuCl_4^-$ with $NaBH_4$. Final partcicle mean radii versus a) ratio of $HAuCl_4$ in binary precursor mixtures of with $KAuCl_4$ and NH_4AuCl_4 at room temperature b) concentration of added NH_4Cl proir or subsequent to reduction at room temperature c)

temperature for heating during synthesis or subsequent to the synthesis.

The observed influences of parameters on the final particle size can be described using the novel growth concept. For electrostatically stabilized particles as investigated herein, colloidal stability is the result of surface charge and therefore dependent on the electrostatic double layer (EDL) and all parameters which affect the EDL[20] for example nature of the present ions including their valency and their hydrodynamic radii.[21] Often, ions with larger radii are expected to form a steric barrier and increase the distance of closest approach for two nanoparticles.[22] However, Wang et al. investigated the critical concentrations required for precipitation of AuNP using different alkali metal ions and showed that the critical concentration does not simply correlate with the size of hydrated cations.[23] H^+, K^+ and NH_4^+ have similar hydrodynamic diameters of about 250-300 pm. The exact determination of the ion radii is very difficult, especially for NH_4^+. In addition, the adsorption behaviour in terms of the gold-ion interaction can be different. Long-chained amines are well known for their strong affinity to charged gold surfaces.[24] The ammonium ion can be assumed to interact differently with AuNP than H^+ or K^+. NH_4^+ leads to significant larger AuNP than H^+ or K^+. In the picture of the growth concept, H^+ and K^+ systems could be illustrated by stability curve A of Figure 3a while NH_4^+ would be illustrated by system B. Precursor mixtures can be assigned to stability curves between A and B resulting in different minimal particle radii between r(A) and r(B). The EDL is also affected by the ionic strength. According to the DLVO theory, high ion concentrations reduce the electrostatic repulsion between charged particles leading to a decrease of colloidal stability.[12]

In the picture of the growth model, an increasing ionic strength can be illustrated by a shift from stability curve A to D. In a first approximation, it does not matter whether the ionic strength is adjusted prior to the synthesis or increased subsequently. If system A describes the standard synthesis leading to a minimal radius r(A) with no added salt , system B could describe the stability curve of a system with increased ionic strength c_x leading to a larger minimal radius r(B). If the ionic strength of system A is increased to c_x subsequently to the synthesis, the stability curve changes from A to B and a new growth step is induced. Hence, the colloidal stability of the final system determines the final particle size. Indeed, subsequent increase of ionic strength results in particles of similar sizes compared to a prior adjustment of ionic strength (see Figure 4b).

In the novel growth concept, the final size is not only determined by the stability curve but also by E_{kT}. An increase of temperature as illustrated in Figure 3b shifts the intersection of thermal energy and stability curve towards larger particle sizes. In the picture of the growth concept, the final particle size has to be approximately the same for a system which is synthesized at T_2 and a system which is synthesized at a lower temperature T_1 and subsequently heated to T_2. The quantity of heating steps is not relevant. However, it should be noted that this is only the case as long as the growth kinetics are much faster than the reduction kinetics as in the case of the herein described AuNP synthesis. As expected from the growth concept, it was found that the AuNP mean radii increase with increasing synthesis temperature. Subsequent heating was shown to result in particles with a similar size to those synthesized directly at a certain temperature with no dependence on the number of heating steps.

Conclusions

The present contribution shows that the growth concept based on colloidal stability which is in contrast to any nucleation model can describe particle formation processes and also illustrate the influences of common parameter variations on the final size. Models which are focused on a nucleation phase at the very beginning of a synthesis cannot explain the influences of parameters during growth and especially how changes subsequent to a synthesis (e.g. heating of an as-synthesized colloidal solution, increase of ionic strength) can induce a later/second particle growth. However, it has to be noted that the final sizes cannot be calculated.

The herein investigated systems are relatively simple compared to most syntheses of colloidal nanoparticles. Herein, colloidal stabilization is only due to electrostatic repulsion forces. Many colloidal systems contain stabilizing agents such as steric stabilizers which also affect the stability curve of a system. In addition, nanoparticle syntheses are typically not characterized by a separation of monomer supply and actual particle growth. Most syntheses comprise a weaker reducing agent (e.g. sodium citrate) so that reduction and growth occur simultaneously throughout the entire synthesis. In these cases, nanoparticle growth is not only due to coalescence. Exemplarily, the growth mechanism of the commonly used Turkevich method is characterized by a seed-mediated growth.[9] However, the minimum particle size in a colloidal solution is in general governed by colloidal rather than thermodynamic stability. Thus, the first relevant size determining step of particle formation (e.g. the formation of seed particles) needs to be described with the colloidal stability approach. For the Turkevich synthesis, this is demonstrated in an upcoming publication.[25] Therefore, this contribution constitutes a first step to describe complex nanoparticle growth processes with a novel growth concept.

Acknowledgements

References

1 B. R. Cuenya, *Thin Solid Films*, 2010, **518**, 3127–3150.

ARTICLE

2 S. E. Lohse and C. J. Murphy, *J. Am. Chem. Soc.*, 2012, **134**, 15607–15620.

3 H. Zhang, M. Jin and Y. Xia, *Angew. Chem.-Int. Ed.*, 2012, **51**, 7656–7673.

4 C. Engelbrekt, P. S. Jensen, K. H. Sørensen, J. Ulstrup and J. Zhang, *J. Phys. Chem. C*, 2013, **117**, 11818–11828.

5 J. van Embden, J. E. Sader, M. Davidson and P. Mulvaney, *J. Phys. Chem. C*, 2009, **113**, 16342–16355.

6 F. Wang, V. N. Richards, S. P. Shields and W. E. Buhro, *Chem. Mater.*, 2013.

7 D. I. Garcia-Gutierrez, L. M. D. Leon-Covian, D. F. Garcia-Gutierrez, M. Treviño-Gonzalez, M. A. Garza-Navarro and S. Sepulveda-Guzman, *J. Nanoparticle Res.*, 2013, **15**, 1–12.

8 H. Zhang, Y. Liu, C. Wang, J. Zhang, H. Sun, M. Li and B. Yang, *ChemPhysChem*, 2008, **9**, 1309–1316.

9 J. Polte, *submitted*, 2015.

10 V. K. LaMer and R. H. Dinegar, *J. Am. Chem. Soc.*, 1950, **72**, 4847–4854.

11 B. Derjaguin and L. Landau, *Zhurnal Eksp. Teor. Fiz.*, 1945, **15**, 663–682.

12 J. T. G. Verwey, *J. Phys. Colloid Chem.*, 1947, **51**, 631–636.

13 E. J. W. Verwey, *Theory of the Stability of Lyophobic Colloids*, Elsevier, Amsterdam, 1948.

14 B. Derjaguin and L. Landau, *Prog. Surf. Sci.*, 1993, **43**, 30–59.

15 J. Polte, R. Erler, A. F. Thünemann, S. Sokolov, T. T. Ahner, K. Rademann, F. Emmerling and R. Kraehnert, *ACS Nano*, 2010, **4**, 1076–1082.

16 J. Polte, X. Tuaev, M. Wuithschick, A. Fischer, A. F. Thuenemann, K. Rademann, R. Kraehnert and F. Emmerling, *ACS Nano*, 2012, **6**, 5791–5802.

17 M. Wuithschick, B. Paul, R. Bienert, A. Sarfraz, U. Vainio, M. Sztucki, R. Kraehnert, P. Strasser, K. Rademann, F. Emmerling and J. Polte, *Chem. Mater.*, 2013, **25**, 4679–4689.

18 F. Kettemann, M. Wuithschick, G. Caputo, R. Kraehnert, N. Pinna, K. Rademann and J. Polte, *CrystEngComm*, 2015, **17**, 1865–1870.

19 H. Kwon, K. K. Kim, J. K. Song and S. M. Park, *Bull. Korean Chem. Soc.*, 2014, **35**, 865–870.

20 L. Ehrl, Z. Jia, H. Wu, M. Lattuada, M. Soos and M. Morbidelli, *Langmuir*, 2009, **25**, 2696–2702.

21 N. R. Dhar and S. Ghosh, *J. Phys. Chem.*, 1926, **30**, 628–642.

22 T. Laaksonen, P. Ahonen, C. Johans and K. Kontturi, *ChemPhysChem*, 2006, **7**, 2143–2149.

23 D. Wang, B. Tejerina, I. Lagzi, B. Kowalczyk and B. A. Grzybowski, *ACS Nano*, 2011, **5**, 530–536.

24 M. Aslam, L. Fu, M. Su, K. Vijayamohanan and V. P. Dravid, *J. Mater. Chem.*, 2004, **14**, 1795–1797.

25 M. Wuithschick, A. Birnbaum, S. Witte, M. Sztucki, U. Vainio, K. Rademann, F. Emmerling, R. Kraehnert and J. Polte, *submitted*, 2015.